Synthesis of Micelle-Templated Silicas from Cetyltrimethylammonium Bromide/ 1,3,5-Trimethylbenzene Micelles

M. Francesca Ottaviani,*,† Alberto Moscatelli,† Delphine Desplantier-Giscard,‡ Francesco Di Renzo,‡ Patricia J. Kooyman,§ Bruno Alonso,|| and Anne Galarneau‡

Institute of Chemical Sciences, University of Urbino, Piazza Rinascimento 6, 61029 Urbino, Italy, Laboratoire de Matériaux Catalytiques et Catalyse en Chimie Organique, UMR 5618 ENSCM−CNRS, 8 rue de l'Ecole Normale, 34296 Montpellier Cedex 5, France, National Center for HREM, Julianalaan 136, 2628 BL Delft, The Netherlands, and CRMHT CNRS 1D, Avenue de la recherche scientifique, 45071 Orléans, France

Received: March 3, 2004; In Final Form: May 31, 2004

Micelle-templated silicas (MTS) were synthesized by self-assembly of inorganic silica and micelles of cetyltrimethylammonium bromide (CTAB) containing different amounts of 1,3,5-trimethylbenzene (TMB) at 343 K. Nitrogen sorption isotherms and transmission electron microscopy (TEM) showed that MTS pore size increased with the increase of TMB amount. However, at TMB/CTAB = 5 the material was characterized by double porosity, due to destabilization of the surfactant emulsion (demixed emulsion), whereas at TMB/CTAB = 13 a stable emulsion originated a solid at uniform pore size. The kinetics of formation of these MTS was followed by inserting a radical-surfactant probe in the surfactant mixture and monitoring, by computer-aided EPR analysis, the structural variations of the surfactant aggregates and of the solid over time. In the absence of TMB, the probes monitored the formation of a polar solid at the surface of the micelles. Only at $t > 150$ min a slow component started contributing to the EPR signal, indicating the formation of the final solid structure. As observed by EPR, at TMB/CTAB = 13, a fast organization of the micelles and a fast condensation of silica accelerated the synthesis process, and in the solid, two probe environments at different polarities were already formed and almost stabilized in the first hour of synthesis. The low polar environment, in which the nitroxide group experienced a relatively high mobility, was attributed to the localization of a portion of TMB in the vicinity of the headgroups of the surfactant aggregates. The proximity of TMB to the silica surface favored and accelerated the formation of siloxane groups. The formation of hydrophobic sites at the surface was also confirmed by ^{1}H NMR, which indicated a lower proton coordination of the surfactants in the presence of TMB, and was further proved on calcined MTS by the decrease in the C_{BET} parameter, which is an indicator of surface polarity. At TMB/CTAB = 5, the kinetics, in the first 100 min of the synthesis monitored by EPR, was equivalent to that found for TMB/CTAB = 13, corresponding to the fast formation of the large porosities. Then, at longer synthesis times, the same slow component as for TMB/CTAB = 0 progressively appeared and contributed to the EPR spectra, corresponding to the final formation of small pores. Therefore, in agreement with the nitrogen sorption isotherms and TEM, the solid formed at TMB/CTAB = 5 is originated by the demixing of the surfactant emulsion into two fractions: the first is TMB-rich and provides a kinetics similar to that of TMB/CTAB = 13; the second is deprived of TMB, providing a kinetics similar to that of TMB/CTAB = 0. Definitely, when TMB is used in the MTS synthesis, the synthesis rate increases and the polarity of MTS surface decreases.

Introduction

Micelle templated silica (MTS) materials[1−6] have attracted much interest in the scientific community for their potential applications in fields of physical chemistry such as catalysis, adsorption, and host−guest chemistry.[7−13] Since they are built from a cooperative assembly of micelles and silicates, these materials possess the unique property of having pores with a uniform size between 20 and 150 Å. Various research groups have studied the formation mechanism of hexagonal MTS in basic media by different techniques using cetyltrimethylammonium bromide (CTAB) as surfactant.[14,15] In this MTS synthesis, two different pathways have been explored:[16−23] the synthesis controlled by hydrolysis of the reactants, which used tetraethoxysilane (TEOS) as a source of silica; and the synthesis controlled by the material organization, which used solid silica and a weak alcalinity.

EPR combined with XRD has been shown to be a powerful tool for following the mechanism of MTS formation.[24−27] EPR probes are radical surfactants that are dissolved in the micelles and provide in situ information about MTS synthesis. Two different synthesis pathways have already been observed by this EPR technique. In the first pathway, using TEOS, Goldfarb and co-workers[24,25] have found a fast formation of hexagonal MTS with the probes strongly interacting with the silica in the first

* Corresponding author: Telephone: +39-0722-4164. Fax: +39-0722-2754. E-mail: ottaviani@uniurb.it.
† University of Urbino.
‡ UMR 5628 ENSCM−CNRS.
§ National Center for HREM.
|| CRMHT CNRS 1D.

10.1021/jp049032p CCC: $27.50
Published on Web 07/21/2004

12−13 min of synthesis, followed by a slow reorganization of the solid. In the second pathway, using dissolved silica,[26,27] a metastable disordered precursor is first obtained, with probes only weakly interacting with silica. Then, this precursor evolves into the final hexagonal MTS, and the signal of probe strongly interacting with the silica surface starts appearing. In the previous study,[26] we have investigated the formation of silicate hexagonal MTS by using cetyltrimethylammonium bromide (CTAB) at 323 K by adding different spin probes to monitor the structural variations of both the micelles and the solid during the synthesis. More recently,[27] the formation of aluminosilicate (Si/Al = 30) hexagonal MTS has been investigated by using alkyltrimethylammonium bromide (nTAB) of different chain lengths to form the starting micelle solutions. These syntheses also passed through the formation of an amorphous material before forming the final hexagonal MTS. Longer alkyl chains lead to faster MTS formation and to stronger interactions between surfactants and silica. This last feature has been explained by a model of hydrophobic corners and hydrophilic sides of MTS hexagonal pores.

In the present study, MTS were obtained by adding 1,3,5-trimethylbenzene (TMB) to cetyltrimethylammonium bromide (CTAB) micelles to increase the pore size of MTS. The kinetics of formation of the structured MTS were followed by introducing 4-cetyldimethylammonium-2,2,6,6-tetramethylpiperidine-*N*-oxide bromide (CAT16) into the CTAB micelles. This probe monitors both the modification of the structure of the CTAB−TMB aggregates and the condensation and organization of the solid silica surface. The probe 5-doxylstearic acid (5DSA), added to the CTAB micelles, was also used to follow the synthesis, but the initial (t = 0 min) EPR signal (not shown) corresponding to a partially ordered material (S = order parameter = 0.4) very poorly changed over the synthesis time when TMB was present in the synthesis mixture. Therefore, the results from this probe were not henceforth discussed in the present study. The EPR spectra were mainly analyzed by the computation of the EPR line shape, extracting parameters indicative of the structural, mobility, and polarity modifications of the surfactant aggregates and the solid over time.

The solid formed at the end of the synthesis was also analyzed by ^{1}H NMR. Nitrogen sorption isotherms and transmission electron micrographs (TEM) were performed to characterize the solid material both as synthesized and after calcination. Nitrogen sorption isotherms provided the pore sizes and volumes, other than the surface areas. Interestingly, it was found that an "intermediate" TMB content (TMB/CTAB = 5) provided two sizes of pores, nicely described by the demixing of the emulsion formed by the TMB−CTAB−water mixture, whereas at high TMB content (TMB/CTAB = 13) only one size of pores was formed, corresponding to a stable emulsion. The EPR results showed that these differently sized pores were formed with a different kinetic. Furthermore, a different solid surface was formed at the various TMB/CTAB ratios, characterized by sites at different polarities.

This study shows how the formation process of the MTS, as well as the nature of the silica surface, can be modified by varying the amounts of TMB added to CTAB aggregates in water solution.

Experimental Section

Materials. The synthesis mixture was prepared by adding the components under stirring, in the following sequence:

1. H_2O, Millipore double distilled (for EPR measurements, a solution of CAT16, kindly provided by Dr. X. Lei, Columbia University, New York, NY, was added at a concentration of 0.1 mM instead of pure water), molar ratio 20;
2. CTAB (Sigma-Aldrich), molar ratio 0.1;
3. NaOH (Sigma-Aldrich), molar ratio 0.25;
4. TMB (Sigma-Aldrich), molar ratio 0−0.5−1.3;
5. SiO_2 (Aerosil 220 by Degussa), molar ratio 1.

After each addition, the mixture was allowed to equilibrate by stirring for 1 min. The final mixture was stirred for 30 min at room temperature and then (a) transferred into an autoclave at 343 K for 5 h and (b) transferred into a glass tube (2 mm diameter) and inserted into the EPR cavity at 343 K. This temperature assured the surviving of the EPR probes during the synthesis time, as guaranteed by the constant EPR intensity.

MTS from process (a) were washed with water and dried at 388 K. After characterization of the as-synthesized MTS, they were calcined at 823 K for 8 h to eliminate the organic matter.

For comparison, CTAB micelle solutions, containing the CAT16 probe at 0.1 mM, were also tested by EPR in the absence and presence of the different amounts of TMB.

Instrumentation. Nitrogen sorption isotherms were performed at 77 K on a Micromeretics ASAP 2010 instrument after degassing samples at 523 K until a stable static vacuum of 3×10^{-3} Torr was reached.

Transmission electron microscopy (TEM) was performed using a Philips CM30T electron microscope with an LaB6 filament at 300 kV. Samples were mounted on a microgrid carbon polymer supported by a copper grid. A few droplets of a suspension of ground sample in ethanol were dropped on the grid and then dried at ambient conditions.

EPR spectra were recorded by means of a EMX-Bruker spectrometer operating at X band (9.5 GHz). The temperature was controlled with a Bruker ST3000 variable-temperature assembly cooled with liquid nitrogen. The samples were inserted in glass tubes of 2 mm diameter. The EPR cavity was held constant at 343 K for the synthesis.

Solid-state NMR spectra were recorded on a Bruker DSX 400 spectrometer by means of 2.5 mm MAS rotors spun at 30 kHz. A single pulse experiment was used for the acquisition of ^{1}H spectra. Radio frequency fields of 50 kHz were employed. Spectra were referenced to TMS.

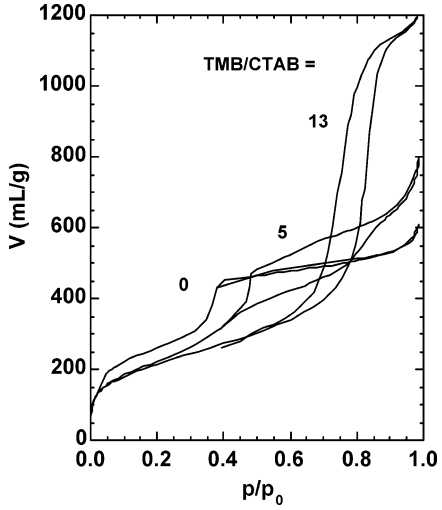

Figure 1. Nitrogen adsorption−desorption isotherms of MTS synthesized at 343 K and then calcined: TMB/CTAB = 0, 5, 13.

Results and Discussion

Characterization of MTS by Nitrogen Sorption Isotherms and TEM. Figure 1 shows the nitrogen isotherms at 77 K of

TABLE 1: Pore Volume (*V*), BET Surface Area (*S*), Pore Diameter (*D*) Determined by BdB Method,[28] and C_{BET} Parameter[a] of Calcined MTS

TMB/CTAB	V (mL/g)	S_{BET} (m^2/g)	D_{BdB} (Å)	C_{BET}
0	0.76	956	39	86
5	0.99	796	41 and 96	69
13	1.90	796	109	70

[a] See text for definition.

MTS synthesized with TMB/CTAB = 0, 5, and 13 at 343 K (same TMB/CTAB ratios and temperature as EPR measurements) and calcined. The isotherms are of type IV (IUPAC classification), showing well-defined cylindrical pores with increasing pore size for MTS synthesized with TMB/CTAB = 0 and 13; the pore filling pressure increases with the amount of TMB. Pore diameters have been evaluated by the Broekhoff and De Boer (BdB) method by using the desorption branch of the isotherm, this method being one of the most suitable to evaluate pore size.[28] Surface area, C_{BET} parameter, pore volume, and pore diameter are reported in Table 1. BET specific surface area and C_{BET} parameter have been calculated in the range $0.06 < p/p_0 < 0.20$, where the BET curves are linear for the samples used in this study. The surface area diminishes from TMB/CTAB = 0 (about 1000 m^2/g) to TMB/CTAB = 5 and 13 (about 900 m^2/g). This implies that the wall thickness of the solids (10 Å) slightly increases with the pore size.[29]

C_{BET} parameter is calculated from the BET equation and is in the first approximation equal to

$$C_{BET} = \exp[(E_{liq} - E_1)/RT]$$

where E_1 is the energy of adsorption of the first layer of nitrogen on the silica surface, and E_{liq} is the energy of adsorption of the following layers of nitrogen often assimilated to the liquefaction energy of nitrogen. Roughly, this parameter is related to the energy of interaction of the nitrogen with the silica surface and therefore allows comparison of the surface polarity of similar materials. $C_{BET} = 100$ is characteristic of a hydrophilic hydroxylated surface of silica, and $C_{BET} = 20$ is characteristic of a hydrophobic silica surface, such as silica grafted with hydrophobic chains.[30] A decrease in surface polarity is notable when TMB is used in MTS synthesis: C_{BET} decreases from 90 to 70, from TMB/CTAB = 0 to 5 or 13. This means that some low polar sites are formed at the silica surface during the synthesis process of MTS using TMB.

As previously described,[31] the increase in pore size and in pore volume of MTS using TMB is not linear versus TMB amount; a minimum amount of TMB/CTAB = 1.6 is necessary to start increasing the pore size. This behavior is nicely due to TMB replacing the hydration water around the ammonium headgroup of the surfactant, because of cation$-\pi$ interactions.[32] A swelling effect of the CTAB aggregates, corresponding to an increase in pore size and pore volume, is well observed in the present study for TMB/CTAB = 5 and 13. However, only the ratio TMB/CTAB = 13 gives rise to a MTS with regular pores of 110 Å diameter, whereas TMB/CTAB = 5 gives rise to a MTS with a double porosity corresponding to the two steps in the isotherm at $p/p_0 = 0.4$ for nonswollen pores of about 41 Å, and $p/p_0 = 0.8$ for swollen pores of about 110 Å. This point is understandable by considering the mixture at high TMB/CTAB ratios as an emulsion. Indeed the synthesis mixture is formed by oil (TMB), water, and surfactant, which form an emulsion. In the phase diagram of an emulsion, for a certain amount of surfactant and oil, the frontiers among emulsion failure, cylindrical phase, and lamellar phase are based on the surfactant/oil volume ratio.[33] A minimum oil volume is therefore necessary to stabilize an emulsion in cylindrical form, and this nicely explains the double porosity at TMB/CTAB = 5 (unstable emulsion) and the uniform porosity of the MTS at TMB/CTAB = 13 (stable emulsion).

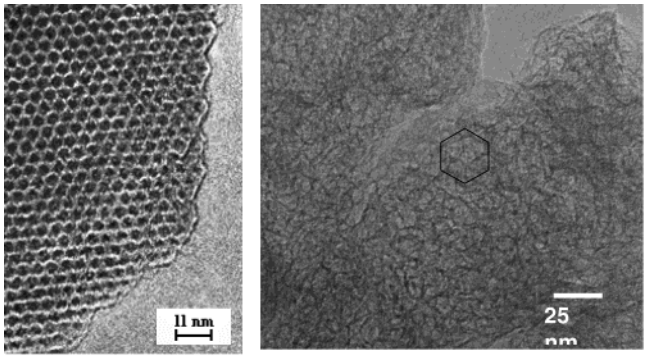

Figure 2. Transition electron micrographs (TEM) of MTS synthesized at 343 K with TMB/CTAB = 0 and 13 and then calcined.

Transmission electronic micrographs (TEM in Figure 2) of the MTS show the same trend observed in the nitrogen adsorption isotherms. MTS materials show homogeneous regular hexagonal pores for TMB/CTAB = 0, whereas the sample synthesized with TMB/CTAB = 13 is a homogeneous large-pore material, where the pores are like soap bubbles touching each other with very thin straight walls (10 Å), forming polygons with six sides of different sizes (disordered hexagon). The sample synthesized at TMB/CTAB = 5 is less homogeneous (TEM not shown) with a part characterized by small pores and another part characterized by large pores.

Unfortunately, X-ray diffraction patterns are not observable for high amounts of TMB since the pore sizes are too large (110 Å).

Definitely the analysis of the nitrogen sorption isotherms and TEM showed that (i) TMB added to the synthesis mixture increases the MTS pore size, but not uniformly and not linearly with TMB content; (ii) the emulsion constituted by TMB−CTAB−water demonstrated instability at TMB/CTAB = 5 (demixing into a TMB-rich portion and a TMB-poor portion, leading to two pore-sized MTS), whereas the emulsion is stable at TMB/CTAB = 13; and (iii) TMB decreased the polarity of the solid surface, because a portion of TMB located around the headgroups of the surfactants and favored silanol condensation. These conclusions are well supported and better motivated by the EPR analysis which follows.

MTS Synthesis Monitored by EPR. The analysis of the EPR spectra is divided into three parts for the three TMB/CTAB ratios (0, 5, and 13; samples with TMB/CTAB = 0 and 13 are discussed before those with TMB/CTAB = 5, since the 5 ratio provides results between 0 and 13 ratios): examples of experimental (full lines) and computed (dashed lines) spectra (computation performed by means of the program of J. Freed and co-workers)[34] are shown in Figure 3 (parts a, b, and c for TMB/CTAB = 0, 5, and 13, respectively). Most spectra are constituted by two components. We performed the computation of the most intense component; then its subtraction from the experimental spectra allowed us to extract and compute the second component (computations also shown in Figure 3). The relative intensities of the two components, which were needed to reproduce the experimental spectra, provided the percentages also reported in Figure 3. The main parameters, extracted from computation and reported in the figure, are the perpendicular

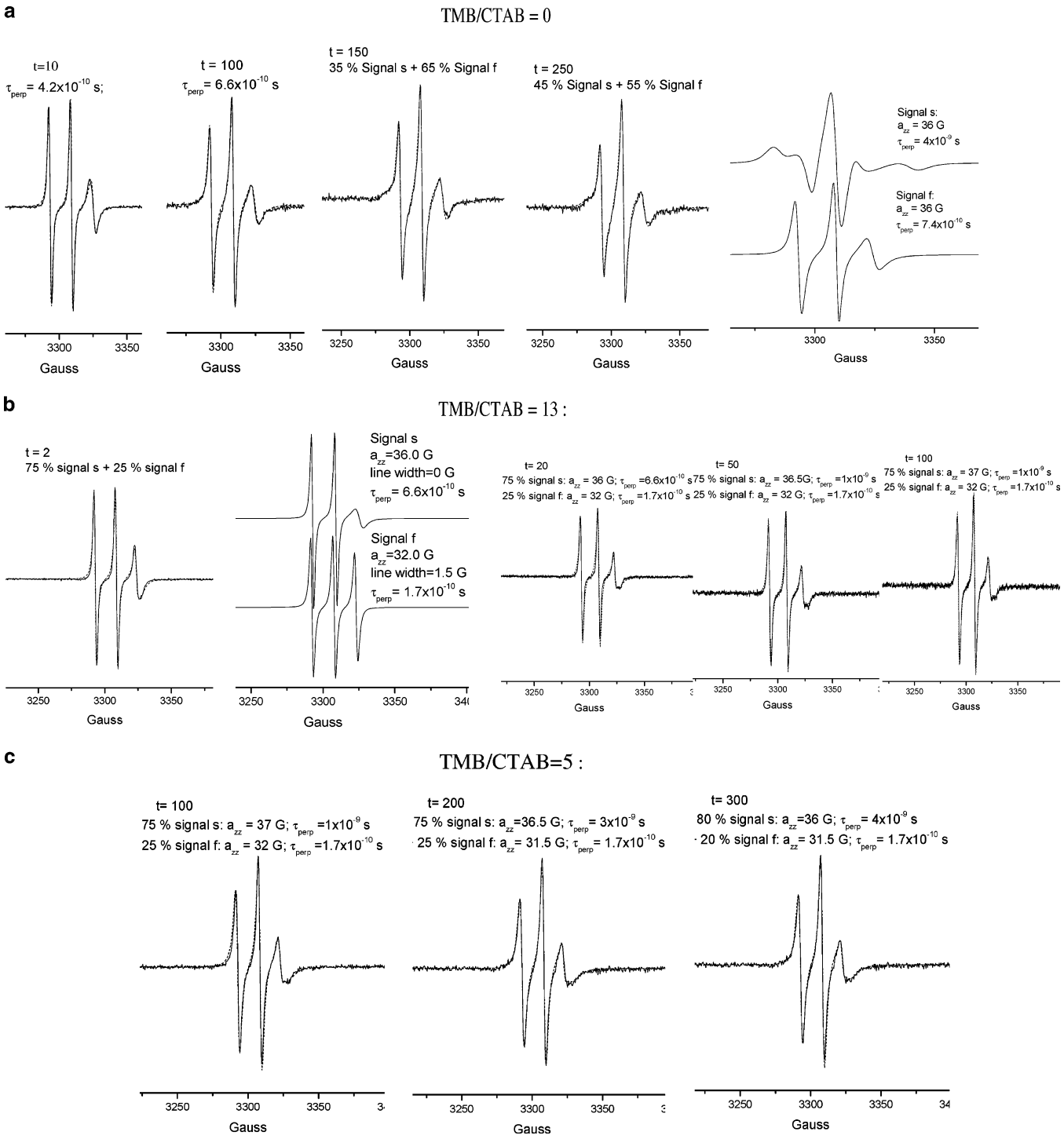

Figure 3. EPR spectra recorded at various synthesis times (probe, CAT16; $T = 343$ K). (a) No TMB; (b) TMB/CTAB = 13; (c) TMB/CTAB = 5. Full lines, experimental spectra; dashed lines, computed spectra. The main parameters used for the computation and relevant for this study (the perpendicular component of the correlation time for motion, τ_{perp}; the a_{zz} component of the hyperfine coupling tensor; the percentage of the spectral component) are indicated in the figure.

component of the correlation time for the rotational diffusion motion, τ_{perp} (accuracy 5%), which decreases with the increase of the probe mobility, and the a_{zz} component of the hyperfine coupling tensor (accuracy 5%), which increases with the increase of the probe environmental polarity. The variation of these parameters, for the MTS synthesis using 0, 5, and 13 TMB/CTAB ratios, are reported in Figure 4 as a function of the synthesis time. The comparison among the graphs in Figure 4 allows extraction of some significant information about the kinetics and the surface properties of the solid which forms.

MTS Synthesis without TMB. Figure 3a shows examples of the EPR spectra recorded at different synthesis times for the micelle−silica systems in the absence of TMB. The experimental spectra are the full lines; the computed spectra are the dashed lines. The line shape changes over time due to a variation in mobility of the probe which monitors the progressive restructuring of the micelles and the solid.

The correlation time evaluated in the first 2−3 min of synthesis (2×10^{-10} s) is the same as that obtained for CAT16 in the CTAB micelles (without silica). Then, the mobility

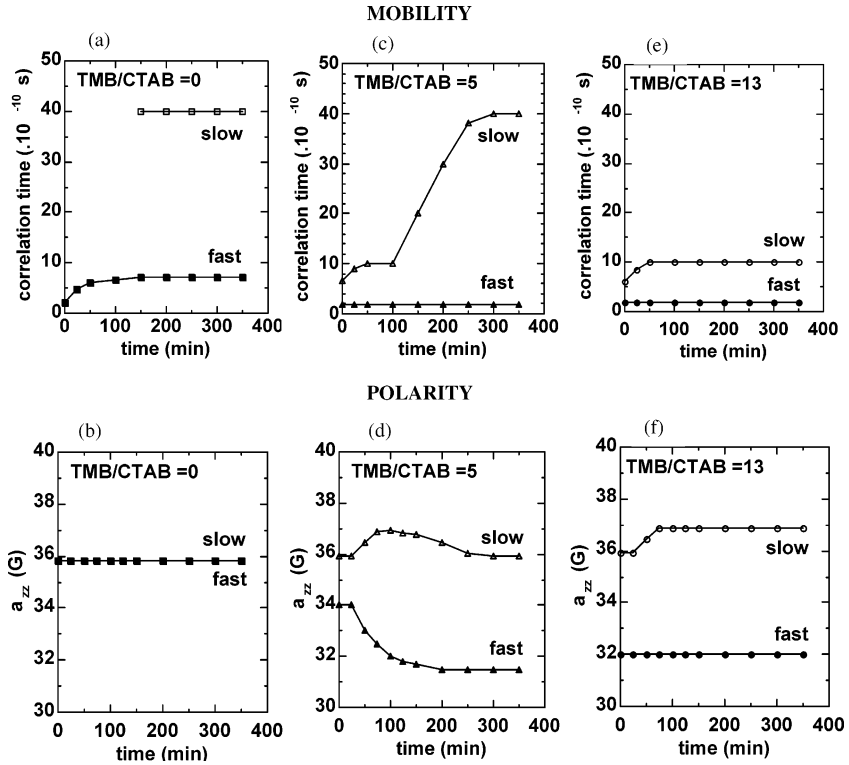

Figure 4. Perpendicular component of the correlation time for motion (τ_{perp}) and zeta component of the hyperfine coupling tensor (a_{zz}), obtained from computation of the slow and fast components constituting the EPR spectra, plotted as a function of synthesis time for TMB/CTAB = 0, 5, and 13.

decreases over time, as plotted in Figure 4a, with a fast decrease in the first 50 min, followed by a slower decrease between 50 and 150 min. However, the variation in mobility is relatively small and this spectral component remains in the so-called fast motion conditions (thereafter called the "fast component"). At $t = 150$ min the mobility of this fast component remains unchanged ($\tau_{perp} = 7 \times 10^{-10}$ s), but, contemporaneously, a second component starts contributing to the spectrum increasing in its relative intensity over time and characterized by a lower mobility ($\tau_{perp} = 4 \times 10^{-9}$ s). This second component, called the "slow component", is due to the direct interaction of the positively charged nitroxide groups, belonging to the probes in the micelles, with the solid surface at the silanol groups. It corresponds to the "interacting component" described in ref 26. The synthesis reported in this previous study was performed at a lower temperature (323 K) with respect to the present study; therefore, the behavior is comparable with respect to the presence of the two components (fast and slow), but the variations in mobility and the kinetics are different for the two synthetic methods.

In summary, the variation of the correlation time of the fast component over time (Figure 4a) is in agreement with a progressive restructuring of the micelle and the solid up to $t =$ 150 min; at this stage the micelles reach their final shape. In the range 150 min $< t <$ 250 min the solid reorganizes in its final hexagonal structure and the percentage of a slow (interacting) component increases over time (but its correlation time for motion remains almost unchanged). However, the synthesis is much faster than reported in ref 26, performed at lower temperature, since at $t = 300$ min the spectral variations become negligible and the final structure was therefore stabilized (with a relative percentage of the slow component of about 40% as in ref 26).

It is noteworthy that the a_{zz} value, as obtained from computation and shown in Figure 4b as a function of the synthesis time, is equivalent for the two components (15.9−16 G). This indicates that the environmental polarity is constant and characteristic of a polar environment, as expected for nitroxide groups surrounded by water and sitting at the silanol groups on the solid surface.

MTS Synthesis with TMB/CTAB = 13. Figure 3b shows some examples of the EPR spectra (experimental and computed) obtained for the MTS synthesis in the presence of TMB/CTAB = 13. Already in the first minutes of synthesis, two components (examples of their computations are also given in Figure 3c) superimpose on each other to originate the overall EPR signals. These components are termed the fast and slow components (the variations of τ_{perp} and a_{zz} as a function of time are reported in parts c and f, respectively, of Figure 4), as in the synthesis without TMB, but their following features are different:

(i) The percentage of the slow component is about 75% at the beginning of the synthesis and it slightly increases (up to 80%) at the end of the synthesis.

(ii) The fast component remains unchanged over the synthesis, characterized by faster mobility ($\tau_{perp} = 1.7 \times 10^{-10}$ s) and lower polarity ($a_{zz} = 32$ G) with respect to the fast component in the absence of TMB. This indicates a fast organization of low interacting−low polar portions of the surface, which does not modify over time. Therefore, the charge heads of the probes feel the presence of TMB, which is partly localized in the vicinity of the charged surfactant heads. This favors the condensation of silanol groups to form low interacting−low polar siloxane groups, as already suggested on the basis of nitrogen sorption results (C_{BET}) on corresponding calcined materials.

(iii) The slow component poorly decreases in mobility (τ_{perp} from 6.6×10^{-10} to 10×10^{-10} s) in the first 50 min of synthesis and has a slight increase in environmental polarity (a_{zz} from 36 to 37 G) in the first 100 min of synthesis. These results indicate a quite fast structuring of the polar part of the solid (in the first

50−100 min) and suggests that the probe heads of the interacting surfactants are in close vicinity to the polar surface sites, but the interaction is much weaker with respect to the MTS synthesized without TMB, since it is perturbed by the presence of TMB at the head level of the surfactants.

MTS Synthesis with TMB/CTAB = 5. Figure 3c shows some examples of the EPR spectra (experimental and computed) obtained for the MTS synthesis in the presence of TMB/CTAB = 5.

The variations of τ_{perp} and a_{zz} as a function of time are reported in parts b and e, respectively, of Figure 4. It is interesting to compare these variations of the parameters with those obtained for TMB/CTAB = 0 and 13. The results show clearly that the synthesis at TMB/CTAB = 5 resembles the synthesis at TMB/CTAB = 13 in the first 100 min, and then it progressively modifies to resemble the synthesis at TMB/CTAB = 0 in the last period of time (250−350 min). This last modification mainly holds for the slow component, whereas the fast component stabilizes at the conditions of the synthesis at TMB/CTAB = 13. All these results are in agreement with the result from surface sorption and TEM, which is the destabilization of the TMB/CTAB/water emulsion to form two phases: (a) a TMB-rich phase which quickly (fast synthesis) originates a solid at large porosity, as found for TMB/CTAB = 13; (b) a TMB-poor phase which slowly (at $t \geq 150$ min) forms a solid at small porosity, as found for TMB/CTAB = 0. However, the low polar fraction of the surface, whose formation is monitored by the fast component, remains unchanged, due to the presence of a fraction of TMB at the polar head level of the surfactants.

In a previous study,[27] we described the site distribution in the hexagonal pores of MTS as characterized by hydrophobic corners, generating the fast EPR component, and hydrophilic sides, generating the slow (interacting) EPR component (Figure 5 of ref 27). These assumptions were proposed by comparing the percentage of slow (interacting) component versus the pore size (in the range of 25−50 Å) of MTS synthesized with alkyltrimethylammonium surfactants with different chain lengths. A correlation has been found in this previous study considering hydrophobic corners of constant size. In the present case, the EPR analysis provides the percentage of the slow component (80%) for MTS synthesized with TMB/CTAB = 13, but the pore size of this as-synthesized MTS could not be calculated geometrically from XRD measurements as in previous work,[27] since the pores are too large to correctly determine the cell parameters. Therefore, a calculation was performed to determine the entire pore diameter (D_p) of this as-synthesized MTS from its apparent pore diameter (D_a), determined by nitrogen sorption isotherm, by means of the equation

$$D_p = D_a(V_p/V_a)^{1/2}$$

where D_a is the diameter of the pore space full of surfactants, determined by the nitrogen filling the pores (BdB method);[28] V_a is the volume of as-synthesized MTS, also determined by nitrogen sorption; and V_p is the total pore volume given by

$$V_p = V_a + V_{CTMA}$$

where V_{CTMA} is the volume of surfactant micelles determined by thermogravimetric analysis and the surfactant density (ρ = 0.77), by the following equation:

$$V_{CTMA} = m_{CTMA}/\rho$$

with m_{CTMA} being the mass of surfactant per gram of silica.

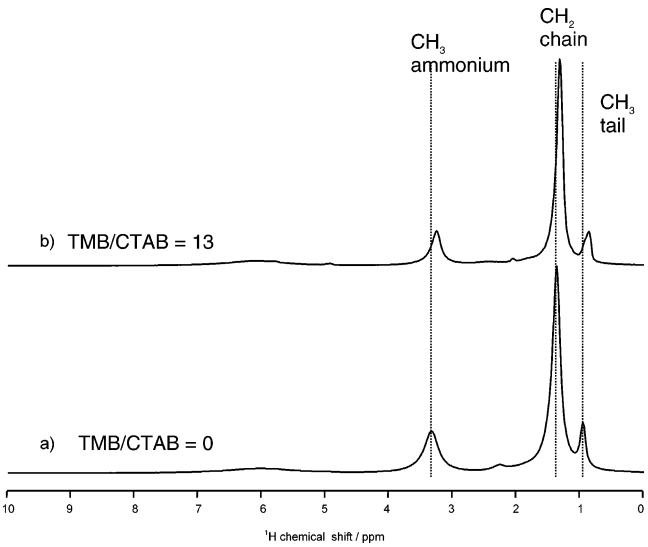

Figure 5. ^{1}H MAS NMR spectra of as-synthesized MTS (synthesis performed at 343 K) at (a) TMB/CTAB = 0 and (b) TMB/CTAB = 13.

This analysis provided a pore diameter (D_p) of 118 Å (which is close to the corresponding calcined materials with a D_p = 110 Å). The percentage of slow component (80%) is lower than expected from the value extrapolated for a pore size of 118 Å in the plot correlating the percentage of slow (interacting) component with the pore size of as-synthesized MTS (Figure 6 of ref 27). Therefore, the fast, low polar component arises from probes interacting not only with the hydrophobic sites at the corners of polygonal pores (distorted hexagon) but also with new hydrophobic sites at the pore sides. The presence of TMB in the synthesis modifies the structure of the pores, creating some less polar sites at the side since water is extruded from the solid surface and some silanols form siloxane groups.

A proof of the effect of TMB on the surfactant−solid interface is provided by the ^{1}H NMR spectra of as-synthesized MTS reported in Figure 5. These spectra clearly show two different environments for quaternary ammonium headgroups in the absence and presence of TMB (TMB/CTAB = 13). The chemical shifts found for the NMR peaks probing the surfactant head, chain, and tail are lower in the presence than in the absence of TMB. This simply means that the surfactant environment has changed by introducing TMB in the synthesis toward a different chain conformation and less interacting protons. Since TMB evaporation created new void spaces, the ordering and structuring of the surfactants were consequently modified. Therefore, the chemical shift probed by the heads for the synthesis in the presence of TMB may arise from a different surface−headgroup interaction, which correlates with the presence of a low polarity environment of the EPR probe, as well as from a different ordering of the surfactant due to the void spaces created by TMB evaporation.

Conclusions

TMB was added to CTAB micellar solutions to increase the pore size of micelle-templated silica obtained by means of an inorganic source of silica. The synthesis was performed at 343 K and at different amounts of TMB. Nitrogen sorption isotherms and TEM were used to analyze the solid obtained at the end of the synthesis. The computer-aided EPR study of the kinetics of formation of the MTS was performed by adding the spin probe CAT16 to the CTAB micelles in the absence and presence of TMB: the analysis was performed for TMB/CTAB = 0, 5, and 13. Mainly the results can be summarized as follows:

1. TMB increases the pore size: nitrogen sorption isotherms and TEM confirmed the formation of homogeneous large pores (110 Å) when a TMB/CTAB = 13 mixture was used, whereas at TMB/CTAB = 5 two sizes of pores were formed.

2. TMB accelerates the kinetics of formation of the solid and provides a rapid structuring of the surfactant aggregates and a fast polymerization of the solid.

3. The TMB/CTAB/water mixture forms an emulsion. Both nitrogen sorption isotherms and EPR analysis indicate that a stable emulsion at TMB/CTAB = 13 quickly forms a large-pore solid, whereas demixing of the emulsion at TMB/CTAB = 5 originates two different pore sizes: a TMB-rich phase produces the large-pore solid and a TMB-poor phase produces the small-pore solid.

4. TMB partly localizes around the headgroups of the surfactants, thus forming a less polar environment at the head level, as monitored by EPR and confirmed by ^{1}H NMR.

5. As a consequence of the localization of TMB at the head level, TMB increases the silanol condensation to form siloxanes, and therefore provides less polar surface sites. The variation of C_{BET} parameter for the calcined MTS confirmed the decrease in surface polarity corresponding to the enhancement of silica condensation by the use of TMB.

The kinetics of TMB formation may be summarized as follows:

At TMB/CTAB = 13, the immediate stabilization of the TMB−CTAB−water emulsion leads to a fast polymerization of the silica and the two hydrophilic and hydrophobic environments of the surfactant heads are already formed and almost stabilized in the first hour of synthesis. For the intermediate TMB/CTAB = 5 ratio, two polymerization steps were found as a function of the synthesis time. The faster polymerization step is similar to that found for the TMB/CTAB = 13 ratio and leads to the fast formation of the large-pore MTS, whereas the slower polymerization step is similar to that found for TMB/CTAB = 0 and leads to the slow formation of the small-pore MTS.

Definitely, the final structuring of the silica is faster in the presence than in the absence of TMB since the solid reorganization is easier, due to already organized siloxane bridges and aggregated surfactants.

In summary, two different procedures allow control of the pore size of the final structure of MTS: the variation of the length of surfactant chain, as described in ref 27, or the addition of organic molecules, such as TMB, that enlarge the surfactant aggregates. The former method does not modify the final surface properties, that is, the distribution of hydrophilic and hydrophobic sites, while the latter does.

Acknowledgment. M.F.O. and A.M. thank the Italian Ministero dell'Università e della Ricerca Scientifica (MURST) and PRIN2002 for their financial support.

References and Notes

(1) Kresge, C. T.; Leonowicz, M. E.; Roth, W. J.; Vartuli, J. C.; Beck, J. S. *Nature* **1992**, *359*, 710.

(2) Beck, J. S.; Vartuli, J. C.; Roth, W. L.; Leonowicz, M. E.; Kresge, C. T.; Schmidt, K. D.; Chu, C. T.-W.; Olson, D. H.; Sheppard, E. W.; McCullen, S. B.; Higgins, J. B.; Schenkler, J. L. *J. Am. Chem. Soc.* **1992**, *114*, 10834.

(3) Inagaki, S.; Fukushima, Y.; Kuroda, K. *J. Chem. Soc., Chem. Commun.* **1993**, 680.

(4) (a) Huo, Q.; Margolese, D. I.; Ciesla, U.; Feng, P.; Gier, T. E.; Sieger, P.; Leon, R.; Petroff, P. M.; Schüth, F.; Stucky, G. D. Nature **1994**, *368*, 317. (b) Huo, Q.; Margolese, D. I.; Ciesla, U.; Demuth, D. G.; Feng, P.; Gier, T. E.; Sieger, P.; Firouzi, A.; Chmelka, B. F.; Schüth, F.; Stucky, G. D. *Chem. Mater.* **1994**, *6*, 1176.

(5) Tanev, P. T.; Pinnavaia, T. J. *Science* **1995**, *271*, 1267.

(6) Bagshaw, S. A.; Prouzet, E.; Pinnavaia, T. J. *Science* **1995**, *269*, 1242.

(7) Armengol, E.; Cano, M. L.; Corma, A.; Garcia, H.; Navarro, M. Y. *J. Chem. Soc., Chem. Commun.* **1995**, 519.

(8) (a) Corma, A.; Martinez, A.; Martinez-Soria, V.; Monton, J. B. *J. Catal.* **1995**, *153*, 25. (b) Corma, A.; Navarro, M. T.; Pariente, J. P. *J. Chem. Soc., Chem. Commun.* **1994**, 147.

(9) Tanev, P. T.; Chibwe, M.; Pinnavaia, T. J. *Nature* **1994**, *368*, 321.

(10) Wu, C. G.; Bein, T. *Science* **1994**, *264*, 1757.

(11) Llewellyn, P. L.; Ciesla, U.; Decher, H.; Stadler, R.; Schüth, F.; Unger, K. *Stud. Surf. Sci. Catal.* **1994**, *84*, 2013.

(12) Branton, P. J.; Hall, P. G.; Sing, K. S. W.; Reichert, H.; Schüth, F.; Unger, K. *J. Chem. Soc., Faraday Trans.* **1994**, *90*, 2821.

(13) Schmidt, R.; Stöcker, M.; Hansen, E.; Akporiaye, D.; Ellestad, O. H. *Microporous Mater.* **1995**, *3*, 443.

(14) Ying, J. Y.; Mehnert, C. P.; Wong, M. S. *Angew. Chem., Int. Ed.* **1999**, *38*, 56.

(15) Patarin, J.; Lebeau, B.; Zana, R. *Curr. Opin. Colloid Interface Sci.* **2002**, *7*, 107.

(16) (a) Chen, C. Y.; Li, H.-X.; Davis, M. E. *Microporous Mater.* **1993**, *2*, 17. (b) Chen, C. Y.; Burkett, S. L.; Li, H.-X.; Davis, M. E. *Microporous Mater.* **1993**, *2*, 27.

(17) Vartuli, J. C.; Schmidt, K. D.; Kresge, C. T.; Roth, W. J.; Leonowicz, M. E.; McCullen, S. B.; Hellring, S. D.; Beck, J. S.; Schenkler, J. L.; Olson, D. H.; Sheppard, E. W. *Chem. Mater.* **1994**, *6*, 2317.

(18) Fyfe, C. A.; Fu, G. *J. Am. Chem. Soc.* **1995**, *117*, 9709.

(19) Firouzi, A.; Kumar, D.; Bull, L. M.; Bessier, T.; Sieger, P.; Huo, Q.; Walker, S. A.; Zasadinski, J. A.; Glinka, C.; Nicol, J.; Margolese, D.; Stucky, G. D.; Chmelka, B. F. *Science* **1995**, *267*, 1138.

(20) Monnier, A.; Schüth, F.; Huo, Q.; Kumar, D.; Margolese, D.; Maxwell, R. S.; Stucky, G. D.; Krishnamamurty, M.; Petroff, P.; Firouzi, A.; Janzationicke, M.; Chmelka, B. F. *Science* **1993**, *1261*, 1299.

(21) Regev, O. *Langmuir* **1996**, *12*, 4940.

(22) Zholobenko, V. L.; Holmes, S. M.; Cundy, C. S.; Dwyer, J. *Microporous Mater.* **1997**, *11*, 83.

(23) Ortlam, A.; Rathousky, J.; Schulz-Ekloff, G.; Zukal, A. *Microporous Mater.* **1996**, *6*, 171.

(24) Zhang, J.; Luz, Z.; Goldfarb, D. *J. Phys. Chem. B* **1997**, *101*, 7087.

(25) (a) Zang, J.; Luz, Z.; Zimmermann, H.; Goldfarb, D. *J. Phys. Chem. B* **2000**, *104*, 279. (b) Zang, J.; Carl, P. J.; Zimmermann, H.; Goldfarb, D. *J. Phys. Chem. B* **2002**, *106*, 5382.

(26) Galarneau, A.; Di Renzo, F.; Fajula, F.; Mollo, L.; Fubini, F.; Ottaviani, M. F. *J. Colloid Interface Sci.* **1998**, *201*, 105.

(27) Ottaviani, M. F.; Galarneau, A.; Desplandier-Giscard, D.; Di Renzo, F.; Fajula, F. *Microporous Mesoporous Mater.* **2001**, *44*, 1.

(28) Galarneau, A.; Desplandier-Giscard, D.; Dutartre, R.; Di Renzo, F. *Microporous Mesoporous Mater.* **1999**, *27*, 297.

(29) Di Renzo, F.; Desplantier, D.; Galarneau, A. *Catal. Today* **2001**, *66*, 75.

(30) Martin, T.; Galarneau, A.; Brunel, D.; Izard, V.; Hulea, H.; Blanc, A. C.; Abramson, S.; Di Renzo, F.; Fajula, F. *Stud. Surf. Sci. Catal.* **2001**, *135*, 29-O-02.

(31) Desplantier-Giscard, D.; Galarneau, A.; Di Renzo, F.; Fajula, F. *Stud. Surf. Sci. Catal.* **2001**, *135*, 06-P-27.

(32) Eriksson, J. C.; Gillberg, G. *Acta Chem. Scand.* **1966**, *20*, 2019.

(33) (a) Gomper, G.; Schick, M. *Self-assembling amphiphilic systems*; Academic Press: London, 1994. (b) Szleifer, I.; Kramer, D.; Ben-Shaul, A.; Gelbart, W. M.; Safran, S. A. *J. Chem. Phys.* **1990**, *92*, 6800.

(34) (a) Schneider, D. J.; Freed, J. H. In *Biological Magnetic Resonance. Spin Labeling. Theory and Applications*; Berliner, L. J., Reuben, J., Eds.; Plenum Press: New York, 1989; Vol. 8, p 1. (b) Budil, D. E.; Lee, S.; Saxena, S.; Freed, J. H. *J. Magn. Reson. A* **1996**, *120*, 155.